

# Pulse plating of Cu-Sn alloy nanoparticles onto gas diffusion layers for the electro-reduction of CO<sub>2</sub>

Lee Fuller

Faculty Sponsor: Sujat Sen, Department of Chemistry and Biochemistry

## ABSTRACT

The electrochemical CO<sub>2</sub> reduction reaction (eCO<sub>2</sub>RR) is slow under ambient conditions, requiring the use of a catalyst in order to reach appreciable rates of conversion. A variety of materials have been explored in the literature, but nano-sized particles of metals such as copper have been shown to generate appreciable amounts of hydrocarbon products such as methane. Furthermore, alloying copper with other metals such as tin has also been demonstrated to tune the selectivity towards more desirable products and minimize the parasitic hydrogen evolution reaction. Herein, we describe the use of direct current and pulsed current methods to successfully deposit nano-sized (< 1 micron) particles of metals such as tin, copper, and their alloys on the surface of commercially available gas diffusion layer (GDL) substrates. Images from a scanning electron microscope (SEM) were used to qualitatively analyze the size and distribution of particles on the surface of the substrate.

## INTRODUCTION

The electrochemical CO<sub>2</sub> reduction reaction (eCO<sub>2</sub>RR) can produce a wide variety of products, including formic acid, methane, ethylene, and carbon monoxide[1]. Some of these chemicals can be used as precursors for plastics and petrochemicals, while others are used as fuels that store energy. When these fuels are burnt for energy, more CO<sub>2</sub> is produced, which can be fed back into the eCO<sub>2</sub>RR, creating a sustainable CO<sub>2</sub> recycling system. Electrochemical CO<sub>2</sub> reduction is advantageous compared to other methods of converting CO<sub>2</sub> because it can be conducted at ambient conditions, and is easy to control the selectivity. Most importantly, electrons are cheap, clean, and efficient [2, 3].

However, the eCO<sub>2</sub>RR is a slow reaction, requiring the use of a catalyst to speed it up. Different types of catalysts used in the eCO<sub>2</sub>RR are known to produce different products. Beginning in the 1980s Hori et al. [4] have demonstrated that many different metals are excellent catalysts for the eCO<sub>2</sub>RR and classified them depending on the majority product formed. For example, metals such as Au, Ag, Zn, Pd, and Ga are selective towards carbon monoxide; Metals such as Pb, Hg, In, Sn, Cd, and Tl are selective towards formate; and metals such as Ni, Fe, Pt, and Ti are selective towards hydrogen, which is a competing reaction in aqueous media. Copper (Cu) is unique because it produces a wide range of products, including methane, ethylene, ethanol, propanol, carbon monoxide, and formate [4]. Since Cu is not selective towards one specific product, it is not an ideal catalyst by itself for large scale applications where separation costs can be high. However, Cu can be alloyed with other metals such as tin to create a catalyst that is selective towards one product [2].

The size of the particle is also known to have a significant effect on catalytic performance [5]. As the particle size decreases, the surface area per unit volume increases, and the effective catalytically active surface area increases. Since the eCO<sub>2</sub>RR is a heterogeneous process, a larger catalytic surface area per unit volume is beneficial. To create nanostructures, the literature has reported several traditional solution-phase methods, which are then physically deposited onto a substrate [6]. Herein, we have investigated the use of electrodeposition as a means to directly generate and deposit nanostructures of metals on the surface of a gas diffusion layer (GDL) substrate.

In electrodeposition, a potentiostat (or any power supply) is used to apply a constant current between the two half cells, cathode, and anode, i.e., galvanostatic operation [7]. As shown in the figure 1, aqueous Cu<sup>2+</sup> ions accept incoming electrons to produce Cu metal, which is deposited onto the cathode. As this reduction process occurs at the cathode, the opposite process of oxidation occurs simultaneously at the anode. At the anode, metallic Cu is stripped off of the anode to produce aqueous Cu<sup>2+</sup> ions. A copper anode was explicitly chosen in this example so it could replenish the ionic solution with aqueous Cu<sup>2+</sup> ions, thereby maintaining constant concentration of depositing ions in

solution. A similar setup is used to deposit copper-tin alloys onto GDL's. Figure 1 depicts a typical electrodeposition setup.

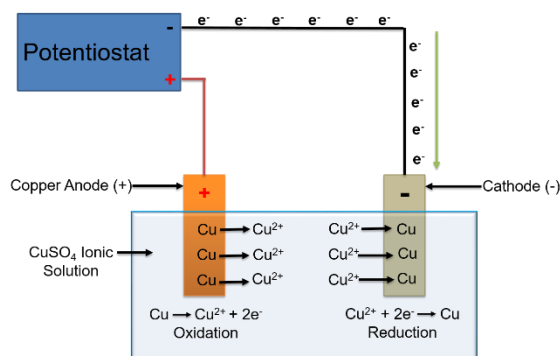


**Figure 1.** Experimental setup showing the cathode, anode, electrolytic solution, and direction of electron movement during electrodeposition.

Two forms of electrodeposition include direct current (DC) electrodeposition and pulse current (PC) electrodeposition [8, 9]. The figure below reflects these two forms of electrodeposition.

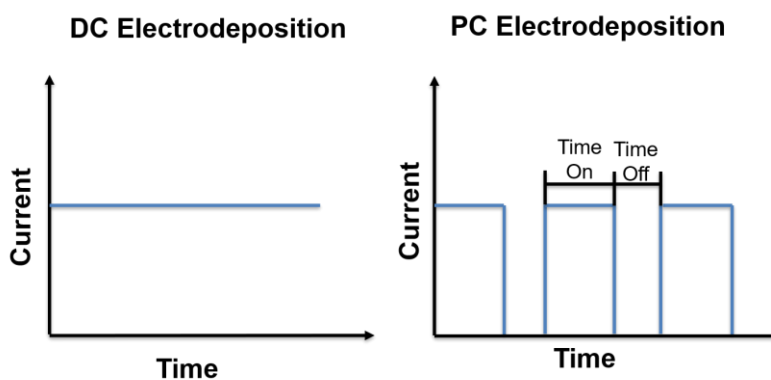


**Figure 2.** Current vs. time profile for (left) direct current (DC) and (right) pulsed current (PC) electrodeposition.

In DC electrodeposition, the current is continuously applied until specific charge densities, and current densities are met. In PC electrodeposition, a constant current is applied for a certain amount of time (time-on), followed by a rest where no current is applied (time-off). This is considered as one cycle. After one cycle completes, another cycle begins, and this repeats until specific parameters such as current density and charge density are met. Using these methods, we have demonstrated the electro-synthesis of catalyst particles smaller than 1 micron, and in select cases, particles with a fine structure smaller than 100 nm with a relatively uniform coverage of the substrate.

## METHODS & MATERIALS

### *Substrate*

In this study, the catalyst was deposited on a commercially available Sigracet 39 BC gas diffusion layer (GDL) substrate (Fuel Cell Store). This substrate has two main layers, namely the microporous layer (MPL) with an approximate thickness of ca.10 microns and the Carbon fiber substrate (CFS) underneath with an approximate thickness of 300 micron. The manufacturer specifies a Teflon concentration of 23% in the MPL and 0% in the CFS. For each experiment, a 2.1 cm by 2.1 cm square was cut from the stock GDL sheet. The mass of each GDL was

recorded before deposition and then again after deposition in order to determine the mass deposited during electrodeposition.

### Electrodeposition Holder

The electrodeposition holder (see figure 3) consists of a current collector wire that is connected to a piece of graphite. The substrate (GDL) is placed on top of the graphite so that current can be conducted between the current collector and the GDL, which acts as the cathode during electrodeposition. The CFS layer of the GDL touches the graphite, while the MPL remains exposed so that metal can be electrodeposited onto it. From there, a rubber gasket and plastic backing are placed on top of the GDL. Using screws and nuts, the rubber gasket and plastic backing were torqued to the plastic holder at 3 lbf.in. This was done to ensure that the CFS layer of the GDL remains dry throughout the electrodeposition process. The inclusion of the rubber gasket ensures a precisely defined electrodeposition area of 4 cm<sup>2</sup>. All parts for the electrodeposition holder were made from polypropylene sheets (1/4 inch, McMaster Carr) and machines using a CNC mill.

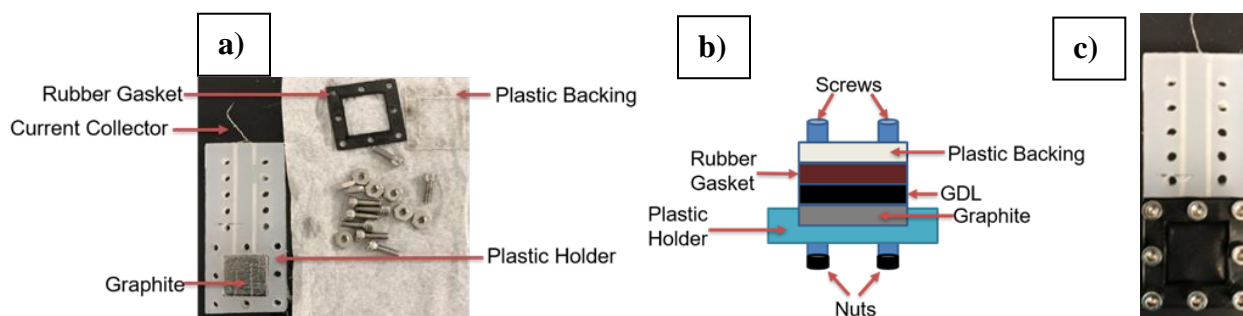


**Figure 3.** (a) Components of electrodeposition holder, (b) schematic of electrodeposition holder assembly, and (c) photograph of a fully assembled electrodeposition holder with MPL facing up.

### Electrodeposition Solution

The tin electrodeposition solution consisted of methanesulfonic acid (MSA) solution (Sigma-Aldrich 70 wt. % in H<sub>2</sub>O) and tin (II) methanesulfonate (Sn-MSA) solution (Sigma-Aldrich 50 wt.% in H<sub>2</sub>O). The MSA was diluted three-fold and was used as a solvent to create a 0.1 M Sn-MSA solution with a starting pH of 0.16. The electrodeposition solution for depositing copper-tin alloys was made by first diluting MSA (Sigma-Aldrich 70 wt. % in H<sub>2</sub>O) three-fold. Then, copper (II) sulfate pentahydrate (CuSO<sub>4</sub>·5H<sub>2</sub>O) (Sigma-Aldrich) and Sn-MSA (Sigma-Aldrich 50 wt. % in H<sub>2</sub>O) were dissolved in the diluted MSA to create a 0.1 M CuSO<sub>4</sub>·5H<sub>2</sub>O and 0.1 M Sn-MSA solution with a starting pH of 0.72. These procedures were adapted from the work of Low et al. [10].

### Run-Time Calculations

Some of the variables involved in PC electrodeposition include charge density at the cathode (C/cm<sup>2</sup>), the current density at the cathode (A/cm<sup>2</sup>), time that current is applied in one cycle (time-on), and time that current is not applied during the same one cycle (time-off) as shown in figure 2. To satisfy the four parameters, a calculation involving these parameters is made to solve for the total run time. This specific total run time ensures that all four desired parameters are met. Inherently, in order to solve for the total run time of PC electrodeposition, one must first solve for the total run time of DC electrodeposition. Calculations for DC electrodeposition and PC electrodeposition are shown below.

### DC Electrodeposition Calculations

DC Electrodeposition Parameters:

Charge Density:  $x$  C/cm<sup>2</sup>

Current Density:  $y$  A/cm<sup>2</sup>

Active Surface Area: 4 cm<sup>2</sup>

1. Charge Density • Active Surface Area = Total Charge  
 $x \text{ C/cm}^2 \cdot 4 \text{ cm}^2 = 4x \text{ C}$
2. Current Density • Active Surface Area = Total Current  
 $y \text{ A/cm}^2 \cdot 4 \text{ cm}^2 = 4y \text{ A}$
3. 1 C is equal to 1 A • 1 s. Therefore, given total current and charge, time ( $t$ ) can be solved for:

$$4x \text{ C} = 4y \text{ A} \cdot t$$

$$t = \frac{4x \text{ C}}{4y \text{ A}}$$

$$t = \frac{4x \text{ A} \cdot \text{s}}{4y \text{ A}}$$

$$t = \frac{x}{y} \text{ s}$$

Therefore, the total run-time for DC electrodeposition is  $\frac{x}{y}$  seconds.

### PC Electrodeposition Calculations

PC Electrodeposition Parameters:

Charge Density:  $x \text{ C/cm}^2$

Current Density:  $y \text{ A/cm}^2$

Active Surface Area:  $4 \text{ cm}^2$

Time-On:  $a$  seconds

Time-Off:  $b$  seconds

1 Cycle = Time-On + Time-Off =  $(a + b)$  seconds

1. Using the same charge density, current density, and Active surface area parameters, solve for the total run-time for DC electrodeposition (see *DC Electrodeposition Calculations* above).
2. The run-time for DC electrodeposition is divided by time-on of PC electrodeposition to solve for the total amount of cycles.

$$\frac{x}{y} \text{ s} \div a \text{ s} = \frac{x}{ya} \text{ cycles}$$

3. The amount of time for one cycle to complete (time-on + time-off) is multiplied by the number of total cycles to find the total run-time for PC electrodeposition.

$$\frac{x}{ya} \cdot (a + b) \text{ s} = \frac{x(a+b)}{ya} \text{ s}$$

Therefore, the total run-time for PC electrodeposition is  $\frac{x(a+b)}{ya}$  seconds.

A Sample calculation is provided below:

Charge Density:  $1 \text{ C/cm}^2$

Current Density:  $0.1 \text{ A/cm}^2$

Active Surface Area:  $4 \text{ cm}^2$

Time-On: 0.01 seconds

Time-Off: 0.09 seconds

$$1 \text{ C/cm}^2 \cdot 4 \text{ cm}^2 = 4 \text{ C}$$

$$0.1 \text{ A/cm}^2 \cdot 4 \text{ cm}^2 = 0.4 \text{ A}$$

$$4 \text{ C} = 0.4 \text{ A} \cdot t$$

$$t = \frac{4 \text{ C}}{0.4 \text{ A}} = \frac{4 \text{ A} \cdot \text{s}}{0.4 \text{ A}} = 10 \text{ s}$$

$$10 \text{ s} \div 0.01 \text{ s} = 1000 \text{ cycles}$$

$$1000 \cdot 0.1 \text{ s} = 100 \text{ s}$$

Therefore, the total run-time for this experiment is 100 seconds.

### Electrodeposition Cell Setup

All electrodeposition runs were carried out in a clean 100 mL glass beaker. A piece of tin (Sn, 99.9%, McMaster Carr) was sanded with fine sandpaper and put in a sonicator for at least 15 minutes, serving as the anode of the

electrodeposition cell. The electrodeposition holder containing the GDL serves as the cathode. After the beaker and the tin anode have been cleaned, the electrodeposition cell was assembled, as shown in figure 4 below. Once the cell has been assembled, it was connected to the DuPR (Dynatronix, MicroStar Series, Model Number: DuPR10-3-6 XR). The negative terminal of the DuPR attaches to the cathode, and the positive terminal of the DuPR attaches to the tin anode.

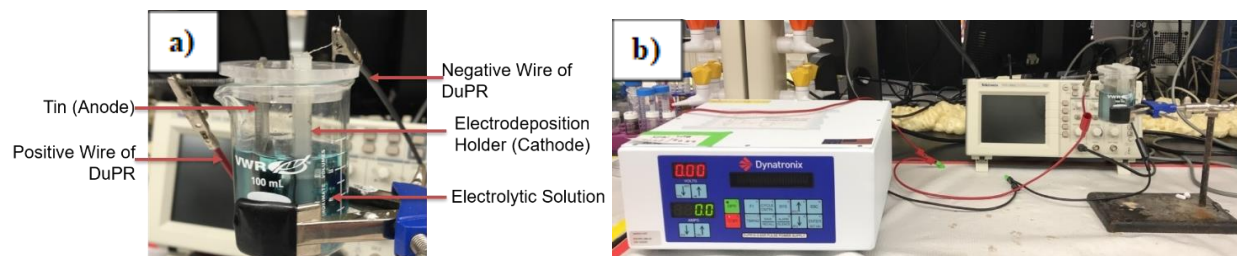


**Figure 4.** The electrodeposition cell is pictured in a), and the DuPR is connected to the cell in b).

### Electrodeposition Experiments

The first type of electrodeposition employed was DC electrodeposition to deposit tin onto GDL's. The table below depicts the parameters used for the DC electrodeposition of tin. The variable that was changed between trials was the current density to see how it affected particle size and the uniformity of coverage on the substrate (see Table 1 below).

**Table 1.** Parameters of DC electrodeposition of tin.

Current Density (mA/cm <sup>2</sup> )	Charge Density (C/cm <sup>2</sup> )	Total Run Time (seconds)
1	2	2000
2.5	2	800
5	2	400
10	2	200
20	2	100
40	2	50
60	2	34
80	2	25

Following DC electrodeposition, PC electrodeposition was used to deposit tin onto GDE's. The main variable that was assessed was current density. Also, time-on and time-off were altered to see if these variables would enhance electrodeposition. Duty cycle (defined as the percent ratio of time-on / (time-on + time-off)) was also considered. Table 2 below depicts the different variables.

**Table 2.** Parameters of PC electrodeposition of tin.

Current Density (mA/cm <sup>2</sup> )	Charge Density (C/cm <sup>2</sup> )	Time-On (milliseconds)	Time-Off (milliseconds)	Total Run Time (seconds)	Duty Cycle (%)
10	1	0.2	9.8	5000	2
100	1	0.2	9.8	500	2
1000	1	0.2	9.8	50	2
10	1	0.5	9.5	2000	2
100	1	0.5	9.5	200	2
1000	1	0.5	9.5	20	2

Lastly, PC electrodeposition was used in efforts to deposit copper-tin alloys onto GDE's. The only variable that was altered between trials was current density (see Table 3).

**Table 3.** Parameters of PC electrodeposition of copper-tin.

Current Density (mA/cm <sup>2</sup> )	Charge Density (C/cm <sup>2</sup> )	Time-On (milliseconds)	Time-Off (milliseconds)	Total Run Time (seconds)	Duty Cycle (%)
1	1	10	90	10000	10
10	1	10	90	1000	10
50	1	10	90	200	10
100	1	10	90	100	10
500	1	10	90	20	10
1000	1	10	90	10	10

### Mass Loading

After electrodeposition was completed, the GDL was let to sit in DI water for five minutes to remove excess electrodeposition solution and subsequently let out to dry in air overnight. After drying, the electrodeposited GDL was weighed in order to determine how much mass was deposited during the experiment. The mass loading of each trial was found by subtracting the mass of the GDL before electrodeposition from the mass of the GDL after electrodeposition. This value was then divided by 4 (area of deposition is 4 cm<sup>2</sup>) to obtain mass loading (mg/cm<sup>2</sup>). Additionally, pictures of the electrodeposited GDE's were taken (iPhone 7) in order to compare the color and coverage of various electrodeposition trials.

### Scanning Electron Microscopy

A scanning electron microscope (SEM) (Zeiss, EVO HD 15) was used to determine the size of electrodeposited particles on GDL's. The typical working distance used to image was 9.5 mm, and the typical accelerating voltage was 10.0 kV.

## RESULTS AND DISCUSSION

### DC Electrodeposition of Tin

The primary tool used to assess the success of each of the trials was the scanning electron microscope (SEM). The first set of trials that were analyzed using SEM were the trials from the DC electrodeposition of tin onto GDL's (see Table 1 above). SEM images of one of these trials are shown below, including scale bars.

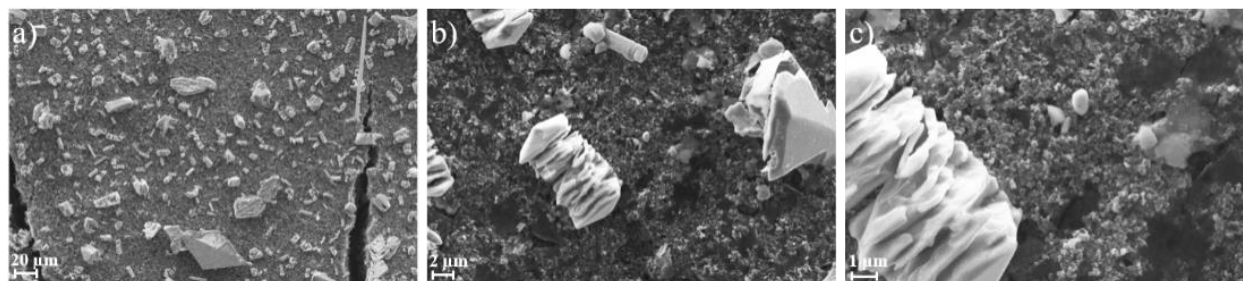


**Figure 5.** SEM images of a GDL electrodeposited with tin via DC electrodeposition. Figure 5a is a 1000x magnification, 5b is a 10000x magnification and 5c is a 25000x magnification. The current density of the trial was 20 mA/cm<sup>2</sup> and the charge density was 2 C/cm<sup>2</sup>. The mass loading was 0.475 mg/cm<sup>2</sup>.

The SEM images in figure 5 show that the DC electrodeposition protocol for that specific trial did not produce nanoparticles. Clearly, many of the solid particles are much larger than 1 μm (or micron). All of the DC electrodeposition trials produced particles similar in size to the particles in figure 5. Therefore, DC electrodeposition was discontinued since it does not readily produce nanostructures.

### PC Electrodeposition of Tin

SEM was used to analyze the PC electrodeposition of tin. Some of these trials are shown in figure 6.

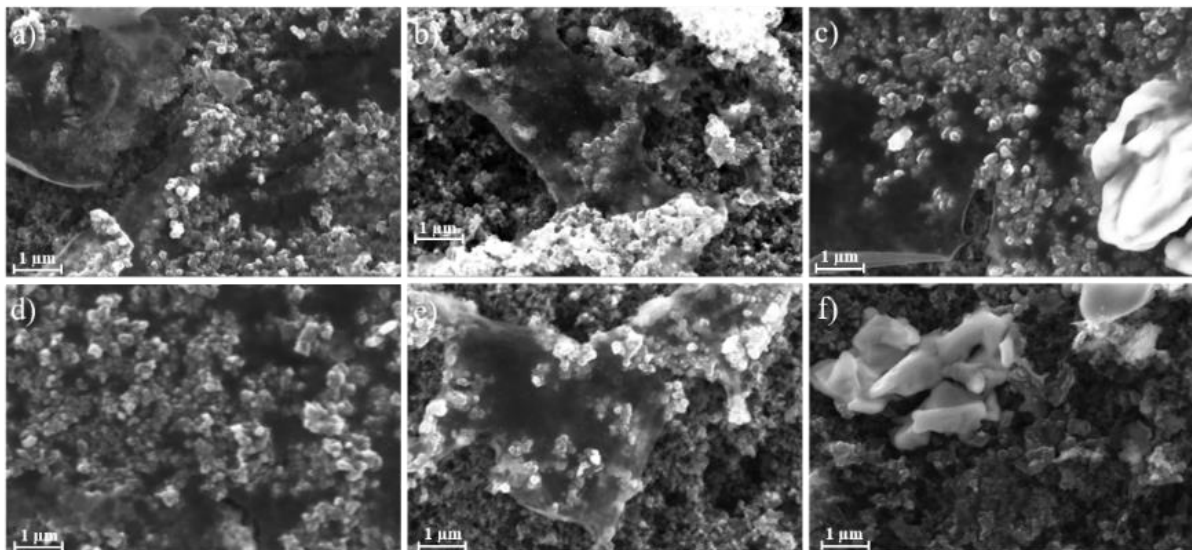


**Figure 6.** SEM images (50000x magnifications) of GDL's electrodeposited with tin via PC electrodeposition. The GDL's in figures 6a, 6b, and 6c were created with a time-on of 0.2 ms and a time-off of 9.8 ms. The GDL's in figures 6d, 6e, and 6f were created with a time-on of 0.5 ms and a time-off of 9.5 ms. Applied current densities are as follows: a) 10 mA/cm<sup>2</sup>, b) 100 mA/cm<sup>2</sup>, c) 1000 mA/cm<sup>2</sup>, d) 10 mA/cm<sup>2</sup>, e) 100 mA/cm<sup>2</sup>, f) 1000 mA/cm<sup>2</sup>.

The PC electrodeposition of tin was difficult because, very often, after electrodeposition, the deposits would fall off of the GDL. This led to difficulties in determining mass loading and accurately analyzing deposition using SEM. Based on the SEM images, there are no clear trends in how current density effects deposition.

### PC Electrodeposition of Copper-Tin Alloys

Finally, GDL's electrodeposited with copper-tin via PC electrodeposition were assessed using SEM, as shown in figure 7. Based on the SEM images taken at 5000x magnification, it is evident that the most uniform-looking and homogenous catalyst developed was the one created at a current density of 100 mA/cm<sup>2</sup> (Figure 7d). The catalyst created at 1 mA/cm<sup>2</sup> (Figure 7a) did not result in many particles. Instead, it resulted in an amorphous deposition. Additionally, SEM images show that the GDL electrodeposited at 1000 mA/cm<sup>2</sup> produced particles as well as amorphous structures. The optical images show that each GDL, besides the one in figure 7a, had relatively uniform deposition across the whole surface area. In order to characterize particle size, even higher magnification SEM images were taken of the GDL's (see figure 8).

With respect to the SEM images taken at 100,000x magnification, increasing current density leads to a decrease in particle size. Between the GDL's created at 10 mA/cm<sup>2</sup> (figure 8b) and 50 mA/cm<sup>2</sup> (figure 8c), it is clear that particle size is smaller in the GDL created at 50 mA/cm<sup>2</sup>. The particles in the GDL created at 50 mA/cm<sup>2</sup> and the particles in the GDL created at 100 mA/cm<sup>2</sup> (figure 8d) are very similar in size. The particles in the GDL created at 500 mA/cm<sup>2</sup> (figure 8e) are smaller than the particles on the GDL created at 100 mA/cm<sup>2</sup>. The size of the particles on the GDL created at 500 mA/cm<sup>2</sup> is similar in size to the particles on the GDL created at 1000 mA/cm<sup>2</sup> (figure 8f). Each of the PC electrodeposition trials resulted in the production of nanoparticles.

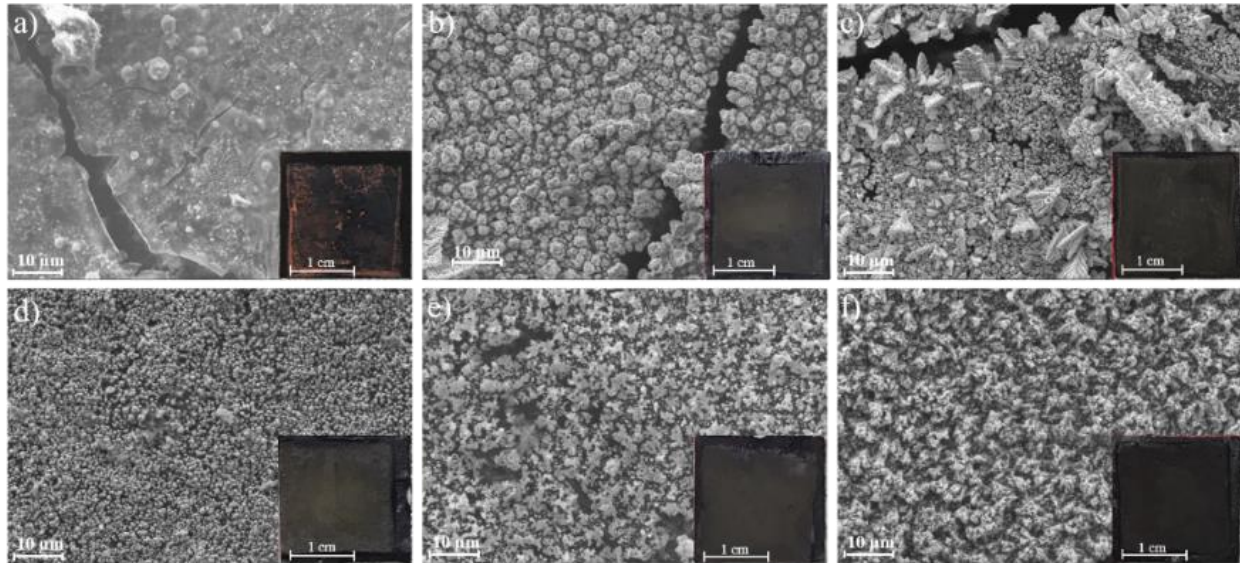


**Figure 7.** SEM (5000x magnification) images of electrodeposition trials created at different current densities: a) 1 mA/cm<sup>2</sup> (mass loading: 0.5 mg/cm<sup>2</sup>), b) 10 mA/cm<sup>2</sup> (mass loading: 1.825 mg/cm<sup>2</sup>), c) 50 mA/cm<sup>2</sup> (mass loading: 0.825 mg/cm<sup>2</sup>), d) 100 mA/cm<sup>2</sup> (mass loading: 0.625 mg/cm<sup>2</sup>), e) 500 mA/cm<sup>2</sup> (mass loading: 0.15 mg/cm<sup>2</sup>), f) 1000 mA/cm<sup>2</sup> (mass loading: 0.7 mg/cm<sup>2</sup>). The inset shows optical images of the same.

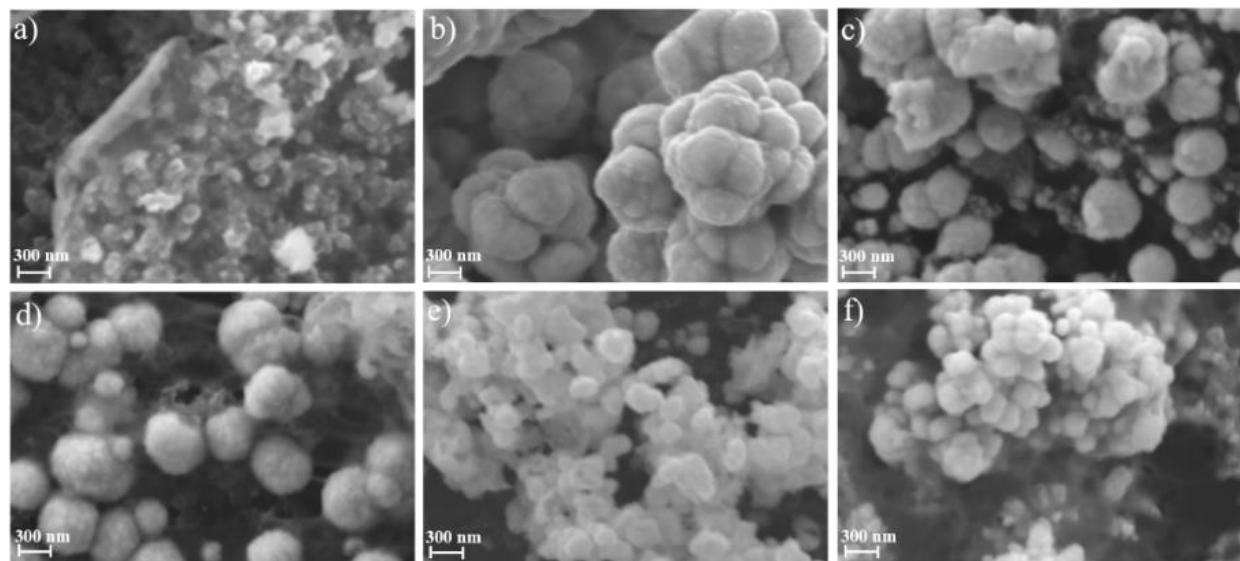


**Figure 8.** SEM (100,000x magnification) images of electrodeposition trials created at different current densities: a) 1 mA/cm<sup>2</sup>, b) 10 mA/cm<sup>2</sup>, c) 50 mA/cm<sup>2</sup>, d) 100 mA/cm<sup>2</sup>, e) 500 mA/cm<sup>2</sup>, f) 1000 mA/cm<sup>2</sup>.

One of the most significant challenges of electrodeposition is reproducibility from run to run. Therefore, trials were repeated to determine reproducibility. In each of the three replication trials (figures 9, 10, and 11), it is evident that as resistance increases a bit (measured between the current collector and GDL), mass loading increases, coverage increases, and particle size decreases. Clearly, inconsistent resistances between trials performed with the

same parameters (current density, time-on, time-off, duty cycle, etc.) results in dramatic differences.

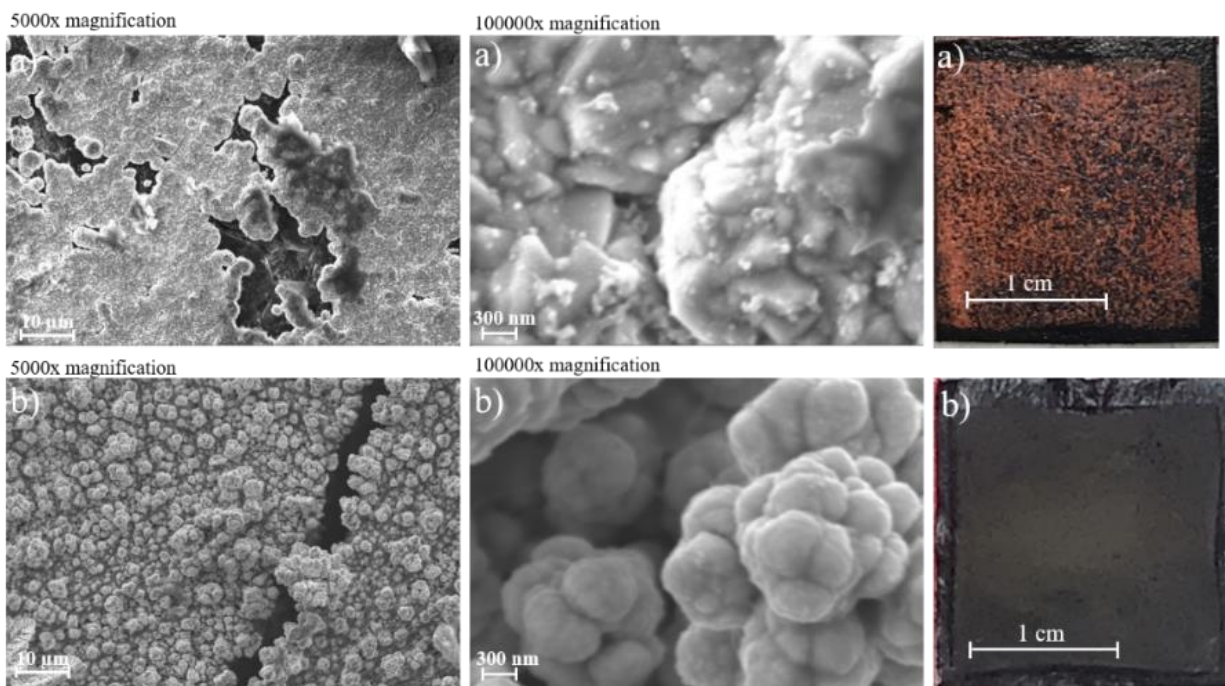


**Figure 9.** SEM and optical images of GDL's that were electrodeposited with the same protocol at a current density of  $10 \text{ mA/cm}^2$ . The resistance of a) and b) before electrodeposition was  $5.8 \Omega$  and  $7 \Omega$  respectively. The mass loading of a) and b) after electrodeposition were  $1.0 \text{ mg/cm}^2$  and  $1.825 \text{ mg/cm}^2$  respectively.

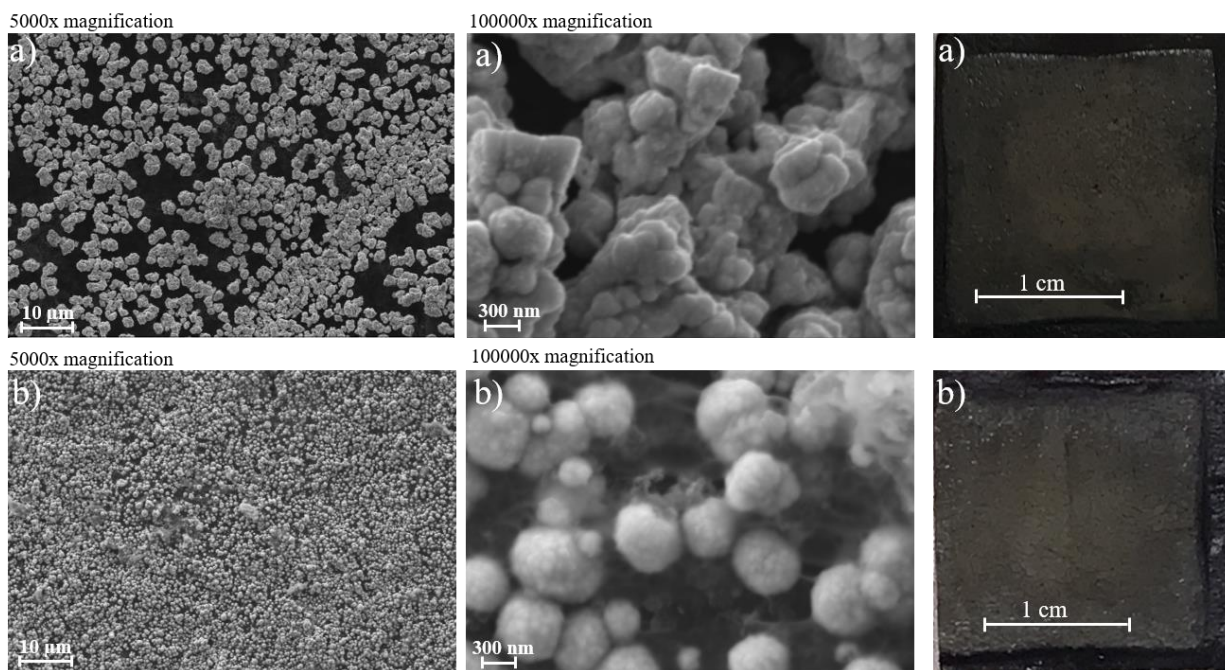


**Figure 10.** SEM and optical images of GDL's that were electrodeposited with the same protocol at a current density of  $100 \text{ mA/cm}^2$ . The resistance of a) and b) before electrodeposition were  $5.1 \Omega$  and  $6.5 \Omega$  respectively. The mass loading of a) and b) after electrodeposition were  $0.475 \text{ mg/cm}^2$  and  $0.625 \text{ mg/cm}^2$  and respectively.

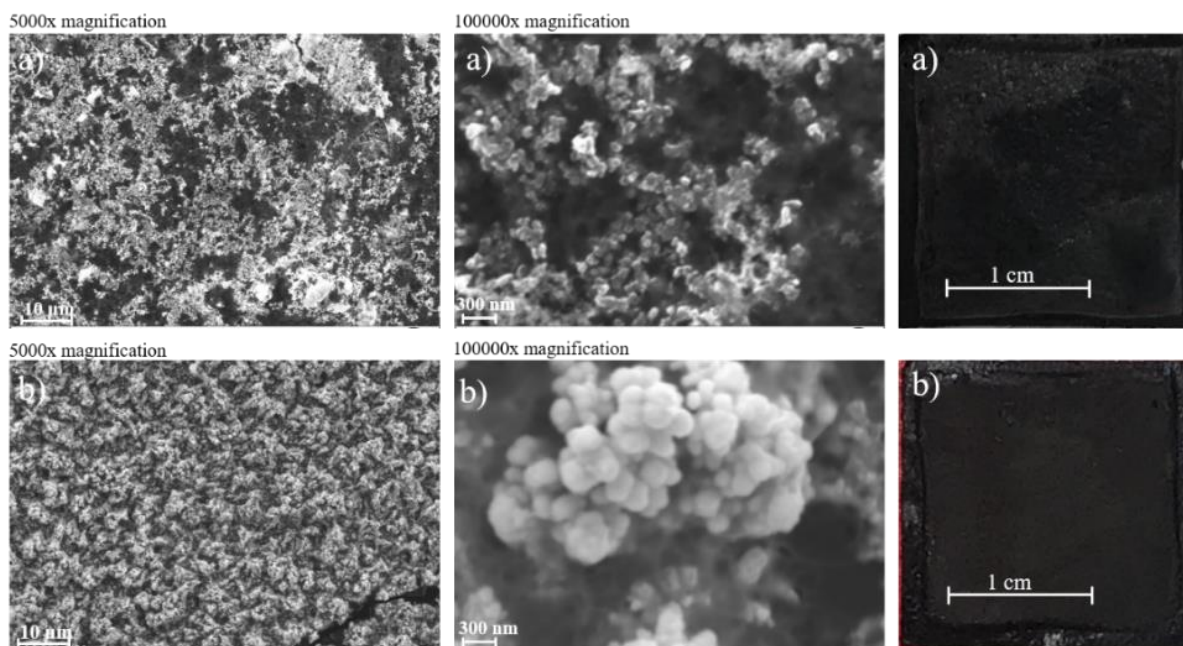


**Figure 11.** SEM and optical images of GDL's that were electrodeposited with the same protocol at a current density of  $1000 \text{ mA/cm}^2$ . Before each electrodeposition trial, each GDL was placed into the electrodeposition holder, and the resistance between the current collector and the GDL was measured. The resistance of a) and b) before electrodeposition was  $4 \Omega$  and  $6.5 \Omega$  respectively. The mass loading of a) and b) after electrodeposition was  $0.15 \text{ mg/cm}^2$  and  $0.7 \text{ mg/cm}^2$  respectively.

## CONCLUSIONS AND FUTURE WORK

As shown in the results section, direct current (DC) electrodeposition of tin does not produce nano-sized particles, but typically results in large micron-sized aggregates that are undesirable from a catalyst point of view. Additionally, pulsed current (PC) electrodeposition of tin was difficult to assess since no trends were evident in SEM imaging. On the other hand, PC electrodeposition of copper-tin alloys showed promising results. Particles with size in the sub-micron and a fine-structure even smaller than  $100 \text{ nm}$  were successfully obtained with uniform coverage on the substrate. It was observed that generally, as current density increased between electrodeposition trials, particle size tended to decrease. However, replication of trials was found to be a persistent issue, likely due to varying resistance between the current collector and the GDL. It was observed that given everything else being equal, as the resistance between the current collector and GDL increased slightly, mass loading increased, coverage increased, and particle size decreased. Future efforts will explore methods to make electrodeposition trials more reproducible, principally by controlling the cathode-to anode distance and the resulting resistance between them. Ongoing efforts into the use of X-ray diffraction (XRD) will reveal the exact composition and identity of the particles deposited. This will reveal if a true alloy has been electrodeposited as opposed to pure tin, pure copper, or some mixture of the two. Electrocatalytic testing of these catalysts for the  $\text{CO}_2$  reduction reaction is ongoing and will be reported elsewhere.

## ACKNOWLEDGEMENTS

Authors would like to thank the office of undergraduate research for funding and support to complete these studies via the URCC 2019 grants, as well as the College of Science and Health for the Dean's Distinguished Fellowship grant. Authors also thank the generous support of the WiSys Applied Research Grants (AR-WiTAG), 2019-2020, and Faculty Research grants, 2019 -2020.

## REFERENCES

- [1] Qi, L., Feng, J., “Electrochemical CO<sub>2</sub> Reduction: Electrocatalyst, Reaction Mechanism, and Process Engineering”, *Nano Energy*, 2016, 29, 439-456.
- [2] (a) Watanabe, M., et al., “Design of Alloy Electrocatalysts for Carbon Dioxide Reduction. III. The Selective and Reversible Reduction of Carbon Dioxide on Copper Alloy Electrodes”, *Journal of the Electrochemical Society*, 1991, 138(11), 3382-3389; (b) Peterson, A.A, Abild-Pedersen, F., Studt, F., Rossmeisl, J., Norskov, J.K., “How copper catalyzes the electroreduction of carbon dioxide into hydrocarbon fuels”, *Energy & Environmental Science*, 2010, 3, 1311-1315.
- [3] Hernandez, S. et al., “Syngas production from electrochemical reduction of CO<sub>2</sub>: current status and prospective implementation”, *Green Chemistry*, 2017, 19, 2326-2346.
- [4] Hori, Y., Murata, A., Takahashi, R., “Formation of Hydrocarbons in the Electrochemical Reduction of Carbon Dioxide at a Copper Electrode in Aqueous Solution”, *J. Chem. Soc., Faraday Trans. I*, 1989, 85(8), 2309-2326.
- [5] Sen, S., Liu, D., Palmore, G.T.R., “Electrochemical Reduction of CO<sub>2</sub> at Copper Nanofoams”, *ACS Catalysis*, 2014, 4, 3091-3095.
- [6] Sen, S., Brown, S.M., Leonard, M., Brushett, F.R., “Electroreduction of carbon dioxide to formate at high current densities using tin and tin oxide gas diffusion electrodes”, *Journal of Applied Chemistry*, 2019, 49, 917-928.
- [7] Hoang, T.T., Ma, S., Gold, J.I., et al., “Nanoporous Copper Films by Additive-Controlled Electrodeposition: CO<sub>2</sub> Reduction Catalysts”, *ACS Catalysis*, 2017, 7, 3313-3321.
- [8] Sen, S., Skinn, B., Hall, T., Inman, M., et al., “Pulsed Electrodeposition of Tin Electrocatalysts onto Gas Diffusion Layers for Carbon Dioxide Reduction to Formate,” *Materials Research Society Advances*, 2017, 2(8), 451-458.
- [9] Leaman, F., “Theory and Practice of Pulse Plating”, *American Electroplaters and Surface Finishers Society*, 1986.
- [10] (a) Walsh, F.C., Low, C.T.J., “A review of the developments in the electrodeposition of tin-copper alloys”, *Surface and Coatings Technology*, 2016, 304, 246-262; (b) Low, C.T.J., Walsh, F.C., “Electrodeposition of tin, copper and tin-copper alloys from a methanesulfonic acid electrolyte containing a perfluorinated cationic surfactant”, *Surface and Coatings Technology*, 2008, 202, 1339-1349.